

# Quantum electron splitter based on two quantum dots attached to leads

A. V. Malyshev,<sup>1,\*</sup> P. A. Orellana,<sup>2</sup> and F. Domínguez-Adame<sup>1</sup>

<sup>1</sup>*Departamento de Física de Materiales, Universidad Complutense, E-28040 Madrid, Spain*

<sup>2</sup>*Departamento de Física, Universidad Católica del Norte, Casilla 1280, Antofagasta, Chile*

Electronic transport properties of two quantum dots side-coupled to a quantum wire are studied by means of the two impurity Anderson Hamiltonian. The conductance is found to be a superposition of a Fano and a Breit-Wigner resonances as a function of the Fermi energy, when the gate voltages of the quantum dots are slightly different. Under this condition, we analyze the time evolution of a Gaussian-shaped superposition of plane waves incoming from the source lead, and found that the wave packet can be splitted into three packets at the drain lead. This spatial pattern manifests in a direct way the peculiarities of the conductance in energy space. We conclude that the device acts as a quantum electron splitter.

PACS numbers: 73.21.La; 85.35.Be; 42.50.Md; 72.90.+y

## I. INTRODUCTION

Quantum dots (QDs) are often referred to as *artificial atoms* since they present discreteness of energy and charge. Moreover, progress in nanofabrication of quantum devices enabled to form an artificial molecule sharing electrons from two or more QDs. In view of the analogy of QDs-based systems and atomic systems, new ways to look for electronic effects are being explored. In this regard, it has been recently demonstrated that coupled QDs shows the electronic counterpart of Fano and Dicke effects that can be controlled via a magnetic flux.<sup>1</sup> In the case of QDs, Fano resonance coexists with Coulomb interaction, giving rise to new quantum transport regimes.<sup>2</sup> In addition, Fano resonances have been clearly observed in a quantum wire (QW) with a side-coupled QD, and it has been proven that this geometry can be used as an accurate interferometer.<sup>3,4</sup>

More recently, we have considered electron transport in a double QD side attached to a QW by means of the two impurity Anderson Hamiltonian.<sup>5</sup> The conductance was found to be a superposition of a Fano and a Breit-Wigner resonances as a function of the Fermi energy, provided the gate voltages of the QDs were slightly different. Remarkably, previous numerical simulations (not shown here) demonstrated that the electron-electron interaction is not responsible of this phenomenon, which can be then regarded as a one-electron process.

In this work we provide further progress along this direction. To be specific, we solve analytically the scattering by the QDs of a wide electronic wave packet moving in the QW, and find that the wave packet can be splitted into three packets after the scattering process, one delayed with respect to the other. Remarkably, this spatial pattern manifests in a direct way the peculiarities on the conductance in energy space. The analytical approach to the problem allows us to understand the dependence of the scattering event on the various parameters of the model. As a result, a fine control of the electron dynamics in the QW can be achieved by changing the gate voltages of the two attached QDs.

## II. CONDUCTANCE AT ZERO TEMPERATURE

The system under consideration is formed by two QDs connected to a QW waveguide, as shown schematically in Fig. 1. The full system is modeled by a two impurity Anderson Hamiltonian, that can be written as<sup>5</sup>

$$\mathcal{H} = -v \sum_{\langle i \neq j \rangle} (c_i^\dagger c_j + c_i c_j^\dagger) - V_0 \sum_{\alpha} (d_{\alpha}^\dagger c_0 + c_0^\dagger d_{\alpha}) + \sum_{\alpha} \varepsilon_{\alpha} d_{\alpha}^\dagger d_{\alpha}, \quad (1)$$

where  $c_i^\dagger$  is the creation operator for an electron at site  $i$  of the QW,  $d_{\alpha}^\dagger$  is the corresponding operator for an electron in the QD  $\alpha = 1, 2$ . The on-site energy of the QW is assumed to be zero and the hoppings are taken to be  $v$ . The hopping  $V_0$  couples the QDs to the QW. Notice that spin indices are omitted hereafter since we do not consider applied magnetic fields or any other interaction breaking spin-degeneracy.

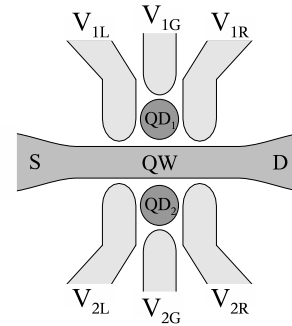


FIG. 1: Schematic view of the two quantum dots attached to quantum wire. Current passing from the source (S) to the drain (D) is controlled by the gate voltages  $V_{1G}$  and  $V_{2G}$ .

The linear conductance can be obtained from the Landauer formula at zero temperature

$$\mathcal{G} = \frac{2e^2}{h} T(\omega = \varepsilon_F), \quad (2)$$

where  $T(\omega)$  is the transmission probability ( $T = |t|^2$ ) with  $t$  the transmission amplitude. The transmission amplitude is given by<sup>6</sup>

$$t(\omega) = 2iv\sqrt{1-\omega^2/4v^2} G_0^W. \quad (3)$$

Here  $G_0^W$  is the Green's function at site 0 of the QW.

By using the Dyson equation we calculate the Green's function at site 0 of the QW coupled to the QDs, obtaining the following expression:

$$G_0^W = \frac{1}{2iv \sin k} \frac{1}{1 - i\eta(g_1 + g_2)}, \quad (4)$$

where  $\eta = V_0^2/2v$ ,  $k = \arccos(-\omega/2v)$ , and  $g_\alpha = 1/(\omega - \epsilon_\alpha)$  ( $\alpha = 1, 2$ ). The transmission amplitude can be obtained from Eq. (3),

$$t(\omega) = \frac{(\omega - \epsilon_1)(\omega - \epsilon_2)}{(\omega - \epsilon_1)(\omega - \epsilon_2) - i\eta(2\omega - \epsilon_1 - \epsilon_2)}. \quad (5)$$

Finally, we arrive at the following expression for the linear conductance at zero temperature

$$\mathcal{G} = \frac{(2e^2/h)(\epsilon_F - \epsilon_1)^2(\epsilon_F - \epsilon_2)^2}{(\epsilon_F - \epsilon_1)^2(\epsilon_F - \epsilon_2)^2 + \eta^2(2\epsilon_F - \epsilon_1 - \epsilon_2)^2}. \quad (6)$$

The density of states of the QDs can give us a better understanding of the transport properties of the system. To obtain it we calculate the diagonal elements of the Green's functions of the QDs. In doing so we obtain<sup>5</sup>

$$\rho = \sum_\alpha \frac{(\eta/\pi)(\omega - \epsilon_\alpha)^2}{(\omega - \epsilon_1)^2(\omega - \epsilon_2)^2 + \eta^2(2\omega - \epsilon_1 - \epsilon_2)^2}. \quad (7)$$

Setting the sites energies as  $\epsilon_1 = \epsilon_0 + \Delta V$  and  $\epsilon_2 = \epsilon_0 - \Delta V$  and taking  $\Delta V \ll \eta$ , we get

$$\rho \approx \frac{2\eta/\pi}{(\omega - \epsilon_0)^2 + 4\eta^2} + \frac{\Delta V^2/2\eta\pi}{(\omega - \epsilon_0)^2 + (\Delta V^2/2\eta)^2}. \quad (8)$$

The density of states is the sum of two Lorentzians with widths  $\Gamma_+ = 2\eta$  and  $\Gamma_- = \Delta V^2/2\eta$ . On the other hand the conductance can be written as

$$\mathcal{G} = \frac{(2e^2/h)\epsilon_F^2}{(\epsilon_F - \epsilon_0)^2 + 4\eta^2} + \frac{(2e^2/h)(\Delta V^2/2\eta)^2}{(\epsilon_F - \epsilon_0)^2 + (\Delta V^2/2\eta)^2}. \quad (9)$$

The conductance is the superposition of the a Fano line shape and a Breit-Wigner line shape. In the limit  $\Delta V \rightarrow 0$  one bound state appears

$$\rho = \frac{1}{\pi} \frac{2\eta}{(\omega - \epsilon_0)^2 + 4\eta^2} + \delta(\omega - \epsilon_0), \quad (10)$$

since one of the states is decoupled from the continuum. A similar effect is already observed in two-channel resonance tunneling.<sup>7</sup> In this limit, the conductance is reduced to a Fano line shape

$$\mathcal{G} = \frac{2e^2}{h} \frac{\epsilon_F^2}{(\epsilon_F - \epsilon_0)^2 + 4\eta^2}. \quad (11)$$

The bound state arises from the indirect coupling of both QDs through the QW, giving rise to level mixing and formation of collective anti-bonded states which have zero amplitude at the QW and are therefore decoupled from it. This mixing arises from quantum interference in the transmission through the two different discrete states (the QD levels) coupled to leads. This result is similar to the Dicke effect in optics, taking place in the spontaneous emission of two closely-lying atoms radiating a photon into the same environment.<sup>8</sup> The coherent indirect coupling of the two energy levels gives rise to the splitting of the decay rates (level broadening), into a fast (superradiant) and a slow (subradiant) mode.<sup>9</sup> Under more realistic experimental conditions when the QW wire has a finite width such state would couple weakly to the QW giving rise to broadening of the  $\delta$ -function in (10).

### III. TIME-DEPENDENT ELECTRON DYNAMICS

Having discussed the steady state properties of the system, we now consider the time-dependent dynamics of electron wave packets. The initial wave packet was chosen to be a narrow Gaussian of width  $a$  in real space, moving in the QW

$$\begin{aligned} \psi_0(x, t) &= \frac{\psi_0}{\sqrt{1 + i\hbar t/ma^2}} \exp \left[ -\frac{(x - v_0 t)^2}{2a^2(1 + i\hbar t/ma^2)} \right] \\ &\times \exp \left[ ik_0 x - i\frac{\hbar k_0^2}{2m} t \right]. \end{aligned} \quad (12)$$

Here the group velocity is  $v_0 = \hbar k_0/m$  and the kinetic energy of the pulse is  $\epsilon_P = \hbar^2 k_0^2/2m$ .

For the sake of clarity, we introduce the following dimensionless variables  $\xi = x/a$  and  $\tau = \hbar t/ma^2$ , as well as the parameter  $\omega_0 = k_0 a$ . In doing so, the wave packet can be rewritten as follows

$$\begin{aligned} \psi_0(\xi, \tau) &= \frac{\psi_0}{\sqrt{1 + i\tau}} \exp \left[ -\frac{(\xi - \omega_0 \tau)^2}{2(1 + i\tau)} \right] \\ &\times \exp [i\omega_0 \xi - i\omega_0^2 \tau/2]. \end{aligned} \quad (13)$$

Following the approach introduced in Ref. 10, the transmitted wave packet after the scattering by the QDs is obtained as

$$\psi(\xi > 0, \tau) \sim \int_0^\infty dq \tilde{\psi}(q) t(q) e^{[iq\xi - iq^2 \tau/2]}. \quad (14a)$$

From Eq. (5) we get approximately

$$t(q) = 1 + \frac{i\Gamma}{q - \omega_0 - i\Gamma} - \frac{i\gamma}{q - \omega_0 + i\gamma}, \quad (14b)$$

where we set  $\epsilon_P = \epsilon_0$ . Here  $\Gamma = 2\eta/\epsilon_0\omega_0$  and  $\gamma = \Delta V^2/2\eta\epsilon_0\omega_0$ . After performing the integration in (14a), the transmitted wave packet is found to be

$$\psi(\xi > 0, \tau) \sim \psi_0(\xi, \tau) + \psi_1(\xi, \tau) + \psi_2(\xi, \tau), \quad (15a)$$

where  $\psi_0(\xi, \tau)$  is the initial wave packet (12) and

$$\begin{aligned} \psi_1(\xi, \tau) = & \sqrt{\frac{\pi}{2}} \gamma \exp[i\omega_0\xi - i\omega_0^2\tau/2] \\ & \times \exp\left[\gamma(\xi - \omega_0\tau) + \frac{\gamma^2}{2}(1 + i\tau)\right] \\ & \times \operatorname{erfc}\left[\frac{\xi - \omega_0\tau + \gamma(1 + i\tau)}{\sqrt{2}\sqrt{1 + i\tau}}\right], \quad (15b) \end{aligned}$$

$\operatorname{erfc}$  being the complementary error function. Moreover,  $-\psi_2(\xi, \tau)$  is obtained from  $\psi_1(\xi, \tau)$  simply replacing  $\gamma$  by  $\Gamma$ . Therefore, it becomes apparent that the scattered wave packet originates from the interference of three contributions, resulting in a complicated spatial pattern as we will show below.

Figure 2 depicts the scattered wave packet at three different values of the dimensionless time  $\tau$ , indicated on each panel. The chosen parameters are  $\gamma = 0.02$  and  $\Gamma = 0.5$ . Hereafter we set  $\epsilon_0 = 2v$ , that is we consider a wave packet centered at the bottom of the QW band where the energy dispersion is quadratic. To improve clarity, both vertical and horizontal axis were scaled, as dispersion makes the wave packet lower and wider on increasing time. We observe that at earlier stages of the scattering process the wave packet splits into two pulses, but after interference with the reflected one, finally a third and much narrowed peak appears at the center.

The width of the third peak is given by  $\gamma$ , as it can be seen from Eq. (15). To show this, one can use the asymptotic form of the complementary error function<sup>11</sup>  $\operatorname{erfc}(z) \approx e^{-z^2}/z\sqrt{\pi}$  ( $z \gg 1$ ) for  $\xi \sim \omega_0\tau$  and  $\gamma\sqrt{\tau}$ ,  $\Gamma\sqrt{\tau} \gg 1$  to obtain

$$\begin{aligned} \psi(\xi > 0, \tau) \sim & \psi_0(\xi, \tau) \left[ 1 + \frac{\gamma(1 + i\tau)}{\xi - \omega_0\tau + \gamma(1 + i\tau)} \right. \\ & \left. - \frac{\Gamma(1 + i\tau)}{\xi - \omega_0\tau + \Gamma(1 + i\tau)} \right]. \quad (16) \end{aligned}$$

The final pattern can be explained from this asymptotic result. The scattered wave packet has two additive contributions, the initial one and a very narrow central peak [two first terms of (16)], while the third term is negative, causing the central and wide dip.

Thus we came to the conclusion that the appearance of the transmitted pulse can be controlled by varying  $\eta$ , namely the effective coupling of the two QDs and the QW, as well as their voltage ( $\Delta V$ ). This result allows for a fine control of the transport properties of the QW with adjusting the parameters of the two QDs. As an example, Fig. 3 the asymptotic wave packet (dimensionless time  $\tau = 20000$ ) for two sets of parameters: a)  $\gamma = 0.0045$  and  $\Gamma = 0.11$ , and b)  $\gamma = 0.045$  and  $\Gamma = 1.1$ . One can notice a change in the spatial pattern by varying the widths of the central peak and the central dip.

The results discussed above refer to two QDs attached to a QW. It is interesting to elucidate the main differences appearing in the scattered pulse with respect to the case of a single QD attached to a QW. Figure 4 shows the

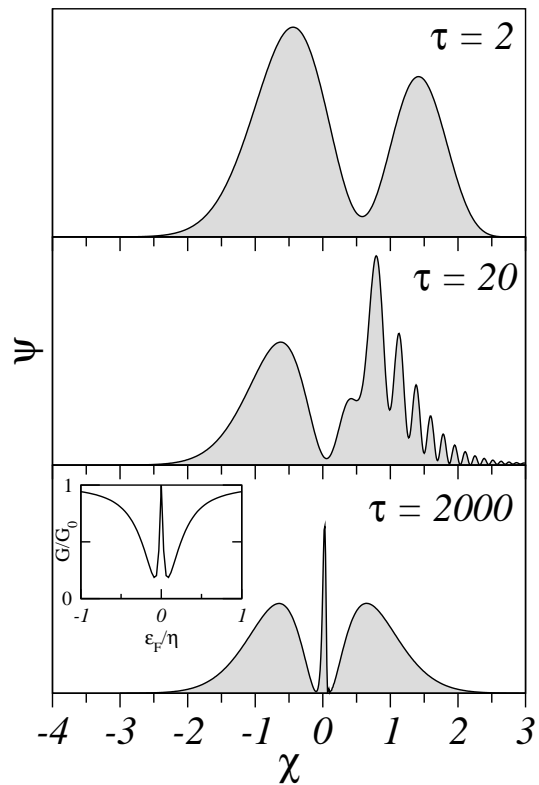


FIG. 2: Scattered wave packet at three different values of the dimensionless time  $\tau$ , indicated on each panel. Vertical axis is scaled by a factor  $\sqrt{1 + \tau^2}$  and  $\chi = (\xi - \omega_0\tau)/\sqrt{1 + \tau^2}$ . The inset shows the corresponding conductance, in units of  $G_0 = 2e^2/h$ , as function of the Fermi energy, in units of the effective coupling  $\eta$ .

asymptotic wave packet (dimensionless time  $\tau = 2000$ ) in both cases. It is clearly seen the vanishing of the central peak after removing one of the two QDs. Notice that this behavior directly reflects the peculiarities of the DOS discussed in Sec. II, in the sense that the narrow Lorentzian peak [second term in Eq. (8)] vanishes when one QD is removed.

#### IV. CONCLUSIONS

We have studied coherent transport through a QW side attached to two QDs with slightly different gate voltages. To this end, a noninteracting two impurity Anderson Hamiltonian was used to describe the electronic properties of the system. We found closed expressions for both the conductance at zero temperature and the density of states. The conductance is the superposition of a Fano line shape and a Breit-Wigner line shape. Also, we found that the density of states is the sum of two Lorentzians of different widths. It resembles the Dicke effect observed in quantum optics. More important, their widths can be controlled via the coupling of the QDs and the QW.

In addition, we analytically solved the scattering of

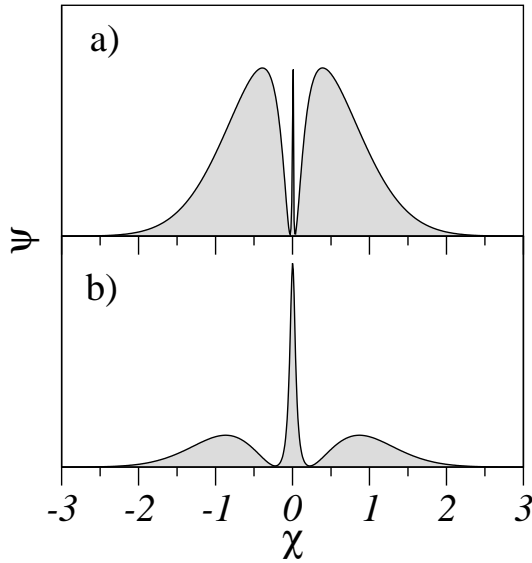


FIG. 3: Scattered wave packet at dimensionless time  $\tau = 20000$  for a)  $\gamma = 0.0045$  and  $\Gamma = 0.11$ , and b)  $\gamma = 0.045$  and  $\Gamma = 1.1$ . Vertical axis is scaled by a factor  $\sqrt{1 + \tau^2}$  and  $\chi = (\xi - \omega_0\tau)/\sqrt{1 + \tau^2}$ .

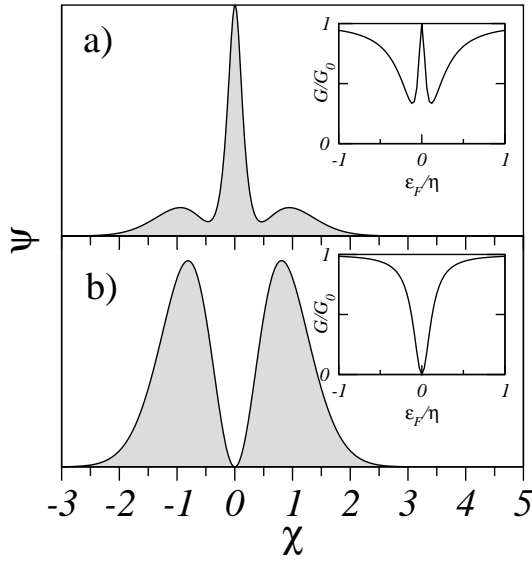


FIG. 4: Scattered wave packet at dimensionless time  $\tau = 2000$  for a) two QDs and b) one QD attached to the QW. Vertical axis is scaled by a factor  $\sqrt{1 + \tau^2}$  and  $\chi = (\xi - \omega_0\tau)/\sqrt{1 + \tau^2}$ . The insets show the corresponding conductance, in units of  $G_0 = 2e^2/h$ , as function of  $\varepsilon_F/\eta$ .

a Gaussian wave packet impinging over the QDs. The scattered wave packet was shown to be the superposition of three pulses, giving rise a complicated pattern as a function of time. In spite of this complex behavior, the long-time asymptotic pulse reflects the peculiarities found in the density of states, showing a central peak whose width can be controlled via the gate voltages. This peak is absent when one of the QD is disconnected from the QW, and the time-dependent current after pulse excitation presents two bumps delayed an amount of  $ma^2/\hbar$ . For couplings between the QDs and the QW of the order of few tenths of meV, and  $a \sim 20$  nm, the delay time might be of the order of few ps in GaAs. To conclude, this phenomenon opens possibilities to design new quantum electron devices like electron splitters, based on physical effects that are usually encountered in quantum optics.

## Acknowledgments

Work at Madrid was supported by MEC (MAT2003-01533). A. V. M. acknowledges financial support of MEC through the Ramón y Cajal program. P. A. O. would like to thank financial support from Milenio ICM P02-054-F and FONDECYT under Grants 1060952 and 7020269. Moreover, P. A. O. would like to thank the hospitality of the Departamento de Física de Materiales of the Universidad Complutense de Madrid during his visit.

\* On leave from Ioffe Institute, St. Petersburg, Russia

<sup>1</sup> P. A. Orellana, M. L. Ladrón de Guevara, and F. Claro, Phys. Rev. B **70** 233315 (2004).

<sup>2</sup> A. C. Jonhson, C. M. Marcus, M. P. Hanson, and A. C. Gossard, Phys. Rev. Lett. **93**, 106803 (2004).

<sup>3</sup> K. Kobayashi, H. Aikawa, A. Sano, S. Katsumoto, and Y.

Iye, Phys. Rev. B **70**, 035319 (2004).

<sup>4</sup> M. Sato, H. Aikawa, K. Kobayashi, S. Katsumoto, and Y. Iye, Phys. Rev. Lett. **95**, 066801 (2005).

<sup>5</sup> P. A. Orellana and F. Domínguez-Adame, phys. stat. sol. (a) **203**, 1178 (2006).

<sup>6</sup> D. S. Fisher and P. A. Lee, Phys. Rev. B **23**, R6851 (1981).

- <sup>7</sup> T. V. Shahbazyan and M. E. Raikh, Phys. Rev. B **49**, 17123 (1994).
- <sup>8</sup> R. H. Dicke, Phys. Rev. **89**, 472 (1953).
- <sup>9</sup> T. Brandes, Phys. **408**, 315 (2005).
- <sup>10</sup> U. Wulf and V. V. Skalozub, Phys. Rev. B **72**, 165331 (2005).
- <sup>11</sup> M. Abramowitz and I. Stegun, *Handbook of Mathematical Functions* (US Government Printing Office, Wahington DC, 1964).